PHYSICAL REVIEW B **78**, 134407 (2008)

Domain fluctuations near the field-induced incommensurate-commensurate phase transition of $TbMnO_3$

H. Barath,[1] M. Kim,[1] S. L. Cooper,[1] P. Abbamonte,[1] E. Fradkin,[1] I. Mahns,[2] M. Rübhausen,[2] N. Aliouane,[3] and D. N. Argyriou[3]

[1]*Department of Physics and Frederick Seitz Materials Research Laboratory, University of Illinois, Urbana, Illinois 61801, USA*

[2]*Institut für Angewandte Physik, Universität Hamburg, Jungiusstraße 11, D-20355 Hamburg, Germany*

[3]*Hahn-Meitner-Institut, Glienicker Strasse 100, Berlin D-14109, Germany*

(Received 16 June 2008; revised manuscript received 11 September 2008; published 10 October 2008)

We present temperature- and field-dependent inelastic light-scattering studies of multiferroic $TbMnO_3$. By carefully examining the evolution of magneto-elastic modes in various phases of $TbMnO_3$, our study reveals several features of the field-induced incommensurate-commensurate (IC-C) transition in $TbMnO_3$. We find that, for fields applied along the *b* axis, there is a coexistence of distinct structural phases in the intermediate field regime ($H=4-7$ T) around the IC-C-phase transition. We present evidence for the existence of dynamical fluctuations of the C phase for fields lower than the critical field for **H** along the *b* axis, $H<H_c^b$. Furthermore, we present evidence for strong spin-lattice coupling effects in $TbMnO_3$ in the form of zone-boundary phonon modes that strongly couple to the spins by modulating the exchange interaction in this material.

DOI: 10.1103/PhysRevB.78.134407 PACS number(s): 75.30.Kz, 75.47.Lx, 75.80.+q, 78.30.−j

I. INTRODUCTION

$TbMnO_3$ is one of several multiferroic materials in which strong magnetoelastic coupling results in an interaction between magnetism and ferroelectricity, and in particular in magnetic-field-induced rearrangements of the polarization vector.[1,2] Several recent studies have demonstrated that this coupling arises from geometrical frustration: the end member of the $RMnO_3$ series, $LaMnO_3$, is known to be an *A*-type antiferromagnet—consisting of ferromagnetically aligned planes of Mn ions that are stacked antiferromagnetically—because of the antiferro-orbital arrangement of the $3d_{3z^2-r^2}$ orbitals.[3,4] However, substitution of La with a smaller trivalent *R* cation leads to a rotation of the MnO_6 octahedra, and a consequent decrease in the nearest-neighbor FM interaction, a suppression of T_N, and frustration of the *A*-type AFM order. For *R*=Gd, Tb, and Dy, *A*-type antiferromagnetic (AFM) order is supplanted by more complex, incommensurate (IC) magnetic order.[3] For example, below a Neel temperature of $T_N\sim 41$ K, $TbMnO_3$ exhibits a longitudinal spin-density wave (SDW) associated with the Mn spins, with a modulation wave vector that is directed along the *b* axis, $k_m^{\mathrm{Mn}}=(0,k+\delta_m^{\mathrm{Mn}},0)$, where the incommensurability $\delta_m^{\mathrm{Mn}}\approx 0.29$ at T_N.[1,5] Accompanying the magnetic ordering is a lattice modulation having $\delta_l=2\delta_m$. At still lower temperatures, below $T_c=28$ K, $TbMnO_3$ exhibits a second transition into a spiral magnetic phase, in which the spins have an elliptic cycloid structure with spins rotating around the *a* axis.[1,5] This phase is associated with the appearance of a spontaneous electric polarization **P** along the *c* axis direction ($\mathbf{P}\|c$) (Refs. 5 and 6) due to an inverse Dzyaloshinski-Moriya coupling between pairs of the noncollinear spins $\mathbf{S}_i$ and $\mathbf{S}_j$ separated by a distance $\mathbf{r}_{ij}$: $\mathbf{P}\propto\mathbf{r}_{ij}\times(\mathbf{S}_i\times\mathbf{S}_j)$. Interestingly, extended x-ray-absorption fine structure (EXAFS) measurements place upper limits on the possible displacements of any atoms in the ferroelectric phase of $TbMnO_3$ at less than 0.005–0.01 Å.[7]

The inherent magnetic frustration and noncollinear magnetic order responsible for multiferroic behavior in $TbMnO_3$ is understandably sensitive to an applied magnetic field, and leads to strong magnetoelastic coupling and hybridized phonon-magnon excitations.[8–10] Recent field-dependent neutron and x-ray diffraction measurements demonstrated that an applied magnetic field above $H_c\sim 4.5$ T (along the *b* axis direction at $T\sim 2.6$ K) relaxes the magnetic frustration caused by the $GdFeO_3$-type distortion.[3] It thereby induces a linear magnetoelastic coupling that drives a magnetostructural transition from an IC phase with $\mathbf{P}\|c$ to a commensurate (C) phase in which **P** flops along the *a* axis, $\mathbf{P}\|a$.[5,6] The critical field, H_c, at which this IC-C transition occurs is a function of temperature, increasing for instance to $H_c\sim 6$ T at $T\sim 10$ K.[2] X-ray diffraction measurements by Aliouane *et al.*[6] showed that, for fields applied along the *b* axis, $\mathbf{H}\|b$, there is a discontinuous transition from the IC to the C phase at 4.5 T that is coincident with the polarization flop. In addition, these measurements demonstrated that there is a coexistence of IC and C phases between 4–5.5 T in $TbMnO_3$ for $\mathbf{H}\|b$ at 2.6 K. The IC-C transition coincides with a ferroelectric polarization flop from $\mathbf{P}\|c$ to $\mathbf{P}\|a$, which is likely driven by the change in the spin-rotation axis of the spiral from the *a* to the *c* axis.[11] This change in the spin-rotation axis requires a degree of magnetic anisotropy that is most likely provided by the rare-earth spins.[11] However, the change to a commensurate phase appears to be accidental, as δ is close to the commensurate value of 1/4. Indeed, $DyMnO_3$ exhibits a field-induced polarization flop $\mathbf{P}\|a$ similar to that in $TbMnO_3$ but this flop is not associated with a commensurate high-field phase.[12] Whatever the exact mechanism of the polarization flop in $TbMnO_3$, the phase coexistence of the IC and C states in the intermediate field regime suggests the possibility of dynamical (fluctuational) contributions to the phase transition that are commonly observed at discontinuous magnetic transitions;[13–15] unfortunately, there has been little or no investigation of $TbMnO_3$ using inelastic-scattering techniques that would be sensitive to the fluctuational dynamics near the temperature- and field-dependent phase transitions of this system.

In this paper, we use inelastic light (Raman) scattering to explore the structural changes and domain fluctuations that accompany the field- and temperature-dependent transitions in $TbMnO_3$. Because it is exquisitely sensitive both to structural order and magnetic degrees of freedom, field-dependent inelastic light-scattering measurements are ideally suited to studying magnetoelastic coupling and multiferroic phases in materials such as $TbMnO_3$.[16–18] Further, by providing information about the energies, intensities, and lifetimes of modes present in different ground states of complex materials, inelastic light scattering provides an excellent means of probing the evolution of both fluctuational and long-lived excitations through pressure- and field-tuned quantum ($T\sim 0$) phase transitions.[19–21] By carefully examining the temperature- and field-dependent evolution of magneto-elastic modes in various phases of $TbMnO_3$, we uncover several features of the IC-C transition in $TbMnO_3$, including: (i) the coexistence of distinct structural phases in the intermediate field regime around the IC-C-phase transition, (ii) the evidence for dynamical fluctuations of the field-induced C phase at fields significantly lower than the established IC-C-phase boundary at H_c, and (iii) evidence for strong magnetoelastic coupling effects associated with the appearance of additional temperature- and field-dependent modes in both the IC and field-induced C phases in $TbMnO_3$. These modes are suggested to be zone-boundary phonon modes that strongly couple to the spins by modulating the exchange interaction in $TbMnO_3$; the intensities of these modes therefore reflect the sublattice magnetization of $TbMnO_3$.

II. EXPERIMENTAL PROCEDURE

The Raman-scattering measurements in this study were performed on $TbMnO_3$ single crystals, which were grown in a floating zone furnace under an Ar atmosphere at the Hahn Meitner Insitut. The phase purity of the crystals was checked by performing x-ray and neutron-diffraction measurements, which indicated that the samples were single phase orthorhombic $TbMnO_3$. The Raman measurements were performed in a true backscattering geometry using the 647.1 nm line from a krypton laser. The incident power was limited to 15 mW with a $\sim$50-μm-diameter laser spot size to reduce laser heating of the sample. Temperature values associated with Raman spectra in this paper include an estimated 5 K contribution associated with laser heating. A modified triple stage spectrometer was used to analyze the spectra. The sample was placed in a variable temperature, pumped Oxford continuous-flow cryostat, which was mounted in the bore of an Oxford superconducting magnet, allowing measurements in the temperature range of 4–350 K and the magnetic-field range of 0–9 T. Magnetic-field measurements were performed in the Voigt geometry with the magnetic-field direction oriented along either the a or b axis crystallographic directions. The incident light was circularly polarized using a Berek compensator to avoid Faraday rotation effects.

III. RESULTS AND DISCUSSION

A. Temperature-dependent spectra

The room-temperature Raman spectrum of $TbMnO_3$ is presented in Fig. 1(a), showing several optical phonon modes in the 110–550 cm^{-1} spectral range, including a number of modes that have been previously observed and identified by Martín-Carrón *et al.*[22] and Iliev and co-workers.[23,24] For example, the 147 cm^{-1} phonon mode in Fig. 1(b) is an A_g-symmetry mode associated with displacements of the Tb^{3+} ions (R mode).[22] In order to explore the low-temperature ($T<T_N$) and field-dependent phases of $TbMnO_3$ in this paper, it is sufficient to focus attention on the Raman spectra between 115–160 cm^{-1}; details of the tem-

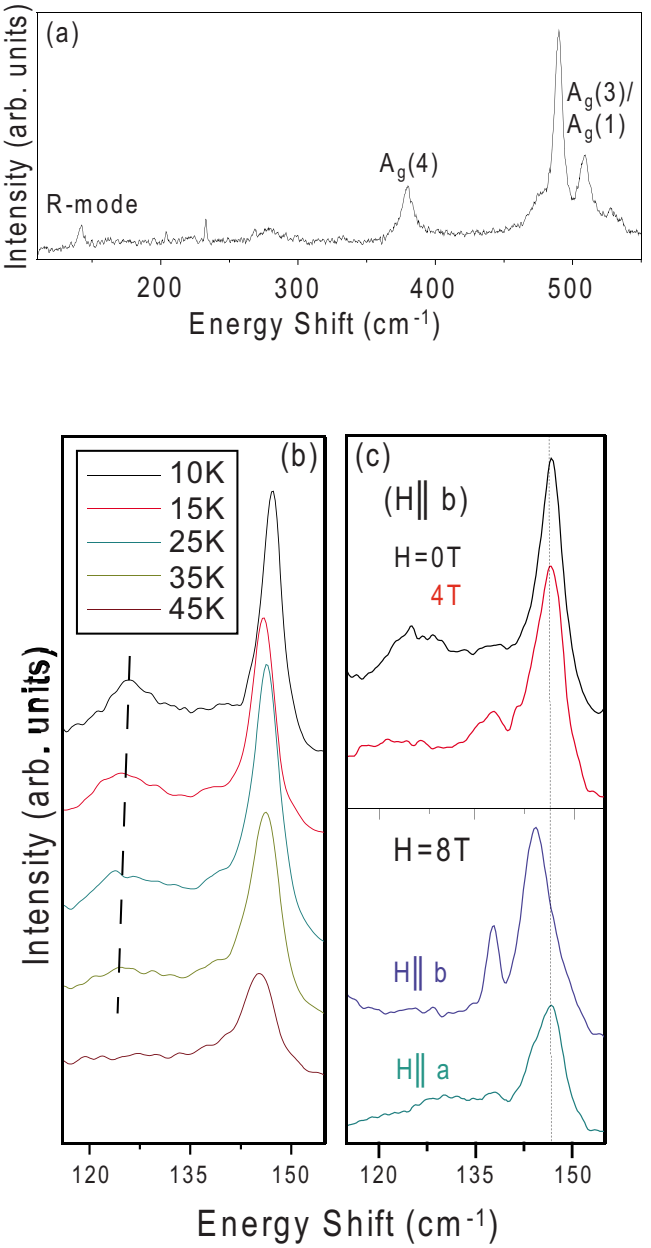

FIG. 1. (Color online) (a) Room temperature Raman spectrum of $TbMnO_3$. (b) Temperature dependence of the zero-field Raman spectra in the 115–155 cm^{-1} spectral range showing the evolution of the IC mode at 125 cm^{-1}; the dashed line is a guide to the eye. (c) Field dependence of $TbMnO_3$ at $T=10$ K for H$\|b$ (top) and H$\|a$ (bottom) axes. The C mode is induced at 137 cm^{-1} for $H>4$ T along the b axis but is not present up to $H=8$ T for applied fields along the a axis.

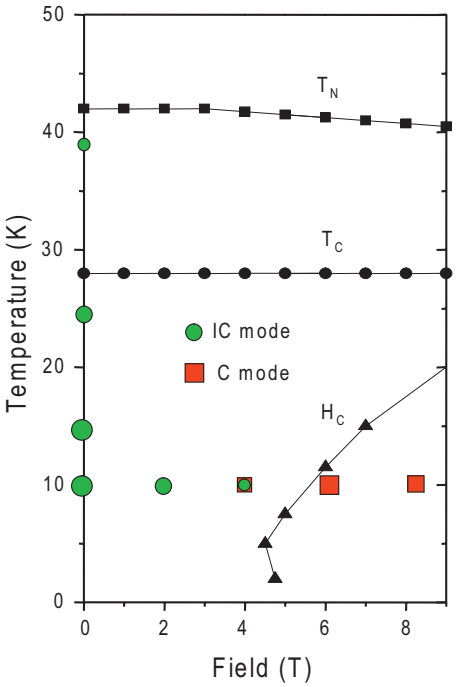

FIG. 2. (Color) The established phase diagram for $TbMnO_3$ (from Ref. 2) overlaid with our data for the IC and C modes, represented by green circles and red squares, respectively. The sizes of the circles and squares provide a rough indication of the relative intensity of the IC and C modes, respectively.

perature and field dependence of the entire phonon spectrum will be published elsewhere.

Figure 1(b) illustrates the temperature dependence of the Raman spectrum in the range of 115–160 cm^{-1}, highlighting several interesting spectroscopic features. For example, Fig. 1(b) shows that a broad mode near 125 cm^{-1} evolves below the transition to the IC longitudinal SDW phase at $T_N \sim 42$ K. We attribute this IC-phase mode to the magnetoelastically induced lattice modulation that accompanies IC magnetic ordering below T_N.[1,2,6] Such a lattice modulation is expected to result in the appearance of modes associated with the incommensurate wave vector of the lattice modulation in $TbMnO_3$ ($\delta_l = 2\delta_m \sim 0.58$ at T_N, where δ_l and δ_m are the lattice and spin incommensurabilities, respectively[6]), as has been observed in the incommensurate phases of other materials.[25,26] In particular, an incommensurate lattice modulation is known to be associated with the appearance of both amplitude and phase vibrational modes;[27] the amplitude mode involves lattice fluctuations that preserve the symmetry of the incommensurate lattice modulation and are therefore Raman active.[25] Our interpretation of the 125 cm^{-1} IC mode as an amplitude fluctuation of the incommensurate lattice modulation is supported by several features of the data: first, the 125 cm^{-1} IC mode softens slightly and broadens as $T \rightarrow T_N$ [dashed line in Fig. 1(b)], as expected of "soft" amplitude modes, and second, the intensity of the 125 cm^{-1} IC mode not only disappears above the IC-phase transition, $T > T_N$, but also disappears with increasing field into the field-induced commensurate C phase [$H = 8$ T spectra in Fig. 1(c)]; the latter is associated with the field-induced destabilization of the lattice modulation that leads to commensuration of the magnetic and atomic lattices above $H_c \sim 5.5$ T at 10 K ($\mathbf{H} \| b$).[6] We also note that the broad linewidth associated with the 125 cm^{-1} IC mode is consistent with inhomogeneous broadening associated with a slight k smearing of the incommensurate wave vector; indeed, a smearing of the incommensurate wave vector in the IC phase of $TbMnO_3$ is supported by the observation that the width of the second-harmonic IC lattice reflection in x-ray diffraction measurements is significantly broader than that associated with the C lattice reflection for $H > H_c^b$.[6]

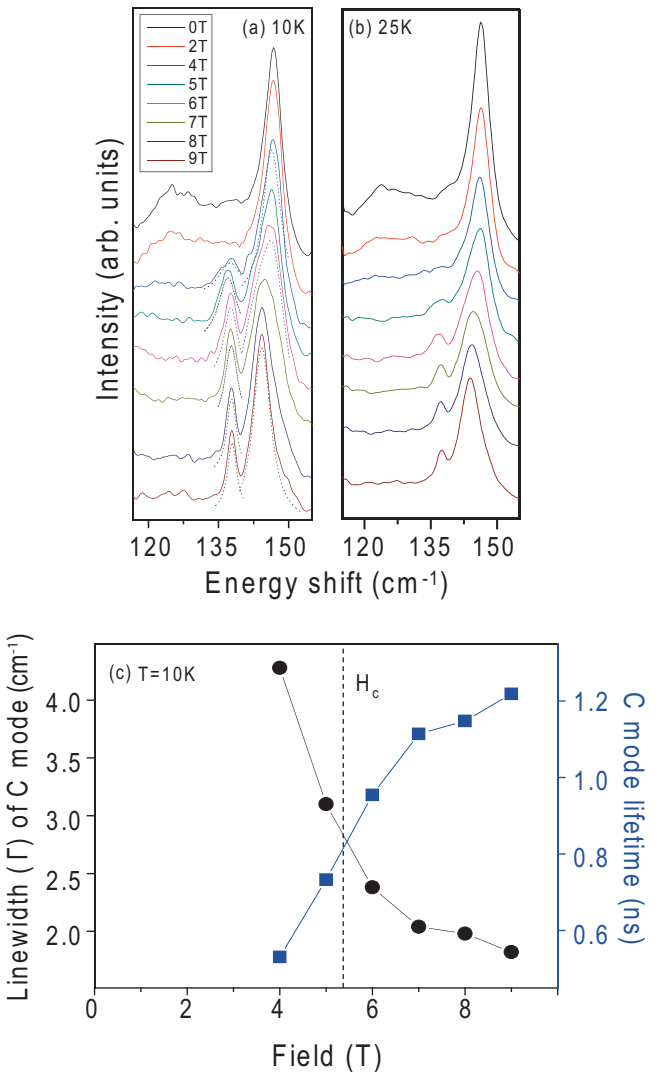

FIG. 3. (Color) Field dependence of $TbMnO_3$ at (a) 10 and (b) 25 K. Dashed lines illustrate Lorentzian fits to the C and 147 cm^{-1} modes, used to extract intensity and linewidth parameters for the C mode. (c) Summary of the linewidth (circles) and lifetime (squares) of the C mode as a function of applied field at $T = 10$ K. The linewidth values include a ~ 0.3 cm^{-1} contribution associated with the instrumental resolution of the instrument.

B. Field-dependent spectra

Figure 1(c) shows that, in addition to a high-field suppression of the IC mode, a narrow field-induced mode near 137 cm^{-1} appears at $H \sim 4$ T for $\mathbf{H} \| b$ in the vicinity of the

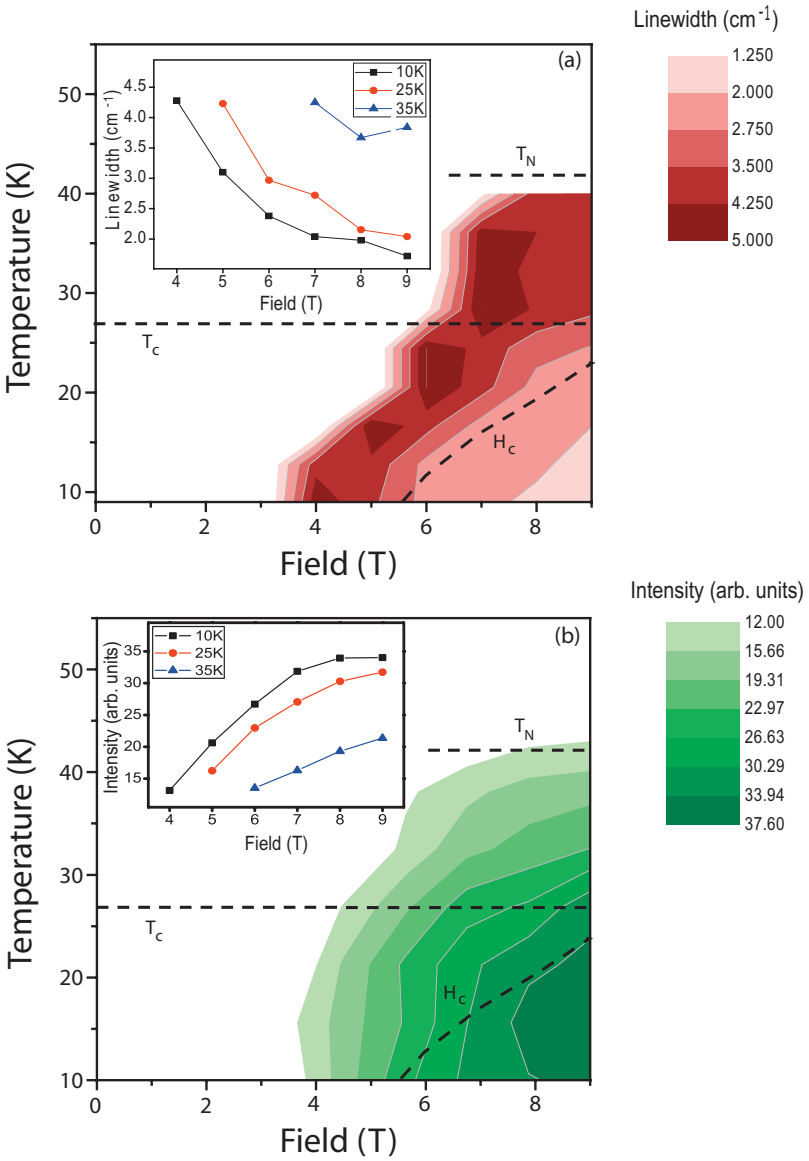

FIG. 4. (Color) Contour plots of the (a) linewidth and (b) intensity of the C mode as a function of temperature and applied field ($\mathbf{H}\|b$). The dashed lines indicate the established phase boundary lines from Ref. 2. The insets shows summary plots of the (a) linewidth and (b) intensity vs field of the C mode at different temperatures.

field-induced IC-C transition. The integrated intensity of this C-phase mode grows with increasing field in the C phase, saturating at $H=6$ T, the field at which the electric polarization flops from $\mathbf{P}\|c$ to $\mathbf{P}\|a$.[1,2] This is shown in Fig. 2, which summarizes some of the temperature and field values at which the IC (green circles) and C (red squares) modes are observed on the established phase diagram of $TbMnO_3$.[2,6] We attribute this C phase near 137 cm^{-1} mode to a zone-boundary phonon mode that is folded to the zone center due to the quadrupling of the unit cell by the magnetic sublattice in the field-induced C phase of $TbMnO_3$.[6] This identification is supported by several features of the data: first, this mode appears near the field-induced IC-C-phase boundary at this temperature, $H_c \sim 5.5$ T, for $\mathbf{H}\|b$. Second, a similar mode is not observed at $H=8$ T in the $\mathbf{H}\|a$ spectra [see bottom spectrum, Fig. 1(c)], in which field orientation the field-induced C phase occurs outside the magnetic-field range of this study, $H_c^a > 9$ T.[6] Finally, the evolution of the field-induced C-phase mode in $TbMnO_3$ is similar to that theoretically predicted for magnetic-order-induced folded phonons[28,29] and experimentally observed in the Raman spectra of magnetic systems such as $RuSr_2GdCu_2O_8$,[30] CuO,[31] and VI_2.[32] In particular, magnetic-order-induced folded Raman modes in these systems are associated with a strong modulation of the exchange coupling constants by specific normal-mode vibrations of the lattice, which contributes a spin dependence to the mode intensity:[28–32] $I_{sd} \sim |M\langle \mathbf{S}_i \cdot \mathbf{S}_j \rangle|^2$, where $\mathbf{S}_i$ and $\mathbf{S}_j$ are the spins on sites i and j, respectively, M is the spin-dependent Raman tensor,[29] and $\langle \ldots \rangle$ represents a statistical average over all lattice sites. Therefore, the presence of these magnetic-order-induced zone-folded modes not only directly illustrates the strong spin-lattice coupling in these materials but the temperature- and field-dependent changes of their intensity directly reflect changes in the sublattice magnetization of the materials. In the specific case of $TbMnO_3$, the rapid growth of the C mode shown in Fig. 3(a) is consistent with that predicted for phonon modes that strongly modulate the exchange coupling of magnetic materials.[29,32] This folded mode may involve longitudinal vibrations of the O ions, as these are expected to strongly modulate ferromagnetic (FM) and AFM exchange couplings in $TbMnO_3$ by modifying the Mn-O-Mn angle.[6]

Because of its sensitivity to the sublattice magnetization of $TbMnO_3$, the field- and temperature-dependent linewidth and intensity of the C mode provides us with an opportunity to identify several interesting properties of the IC-C transition in $TbMnO_3$. Figure 3 presents the detailed field dependence ($\mathbf{H}\|b$) of the IC and C modes at two temperatures (a) $T=10$ and (b) 25 K. With increasing magnetic field, the 125 cm^{-1} IC mode is suppressed while the 137 cm^{-1} C mode appears near the IC/C-phase boundary ($H_c \sim 5.5$ T at 10 K), exhibiting a systematic decrease in linewidth and an increase in intensity with increasing field, as illustrated in Fig. 3(c). The linewidth and intensity of the C mode was extracted from Lorentzian fits to the C and 147 cm^{-1} modes; these fits are illustrated for some select fields as dashed lines in Fig. 3(a). Additionally, there is a dramatic softening in the A_g symmetry Tb mode with increasing magnetic field from $\sim$147 cm^{-1} in the low-field IC phase to $\sim$144 cm^{-1} in the high-field C phase. This softening indicates that there is a structural change, likely involving the Tb^{3+} ions, through the field-tuned IC-C-phase transition. The exact nature of this structural transition is not clear from our data but it may reflect an abrupt change in the lattice modulation associated with the Tb ions through the field-induced IC-C transition. Interestingly, x-ray scattering provides evidence for a strong coupling between the Tb and Mn sublattices below T_c (Ref. 33) so it is likely that this change in modulation through the IC-C transition in $TbMnO_3$ affects the Mn ions as well.

Notably, the field dependence of the C mode intensity and linewidth also provides strong evidence for fluctuating C-phase domain regions that appear at magnetic fields and temperatures well outside the established IC-C-phase boundary, $H_c \sim 5.5$ T (at 10 K). This is illustrated by plotting the C mode linewidth [Fig. 3(c)] and intensity [inset of Fig. 4(b)] for $T=10$ K, which shows that for $H>H_c$ the C mode is strong, with a resolution-limited linewidth, indicative of a long-lived excitation and the presence of long-range commensurate order. However, in the vicinity of the field-induced IC/C-phase boundary, the C mode has a weak intensity and a linewidth three to four times its resolution-limited value. Taken together, these results suggest that the onset of long-range commensurate order at the critical field, H_c, in $TbMnO_3$ is preceded at lower fields by fluctuations of commensurate domains that coexist with incommensurate domain regions near the IC/C-phase boundary of $TbMnO_3$. A similar dynamical coexistence of phases has also been observed using Raman scattering near the quantum neutral-ionic phase transition of isostructural charge-transfer complexes[21] and near the x-dependent quantum ($T\sim 0$) charge-density-wave/superconductor transition of Cu_xTiSe_2.[34]

Figure 4 illustrates the wide range of the phase diagram over which dynamical fluctuations of domains are evident in $TbMnO_3$. Specifically, Fig. 4 shows contour plots of the $\sim$137 cm^{-1} C mode (a) linewidth and (b) integrated intensity as functions of both magnetic field and temperature. Shown in the inset of Fig. 4(a) are the linewidths as a function of applied field at several different temperatures. Also shown for comparison are the established phase boundary lines for the $TbMnO_3$ system (dashed lines) from Ref. 2. The noteworthy features of Fig. 4 are the following: first, the C mode attains its maximum value and has a resolution-limited linewidth inside the established C-phase boundary line, again indicating the presence of long-range commensurate order. However, a fluctuational C mode contribution—characterized by an enhanced linewidth (darker red regions) and weakened intensity (lighter green regions)—is clearly evident outside the established IC/C-phase boundary line, suggesting the presence of fluctuating C domains over a wide range of the phase diagram. These results suggest that, with increasing magnetic field, the C phase nucleates as small fluctuating domains well before the thermodynamic phase transition, and that these C-phase domains become more long-lived and prevalent as $H\rightarrow H_c$, the field at which long-range commensurate magnetic order develops. Significantly, this evidence for field-induced domain formation in $TbMnO_3$ is supported by recent field-dependent neutron-scattering results on $TbMnO_3$, in which an observed memory effect has been attributed to the formation of commensurate domains.[35] These neutron results further suggest that the C-phase domains are associated with a field-induced flop of the spiral plane from the bc plane in the IC phase to the ab plane. In combination with our evidence for fluctuating domains, these results suggest that strong polarization fluctuations likely ac-

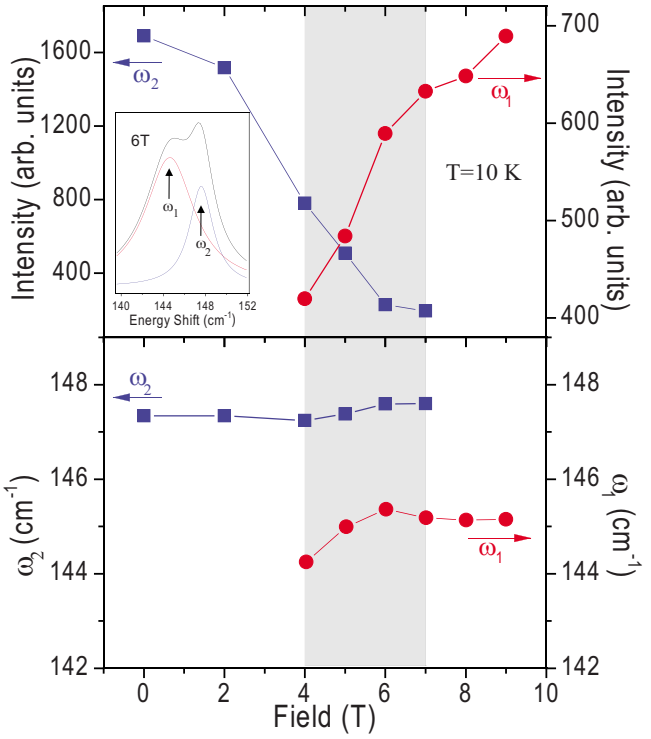

FIG. 5. (Color online) Field dependence (at $T=10$ K) of the (a) integrated intensity and (b) frequency of the A_g symmetry Tb-phonon mode associated with the IC phase (blue squares), where the phonon frequency is $\sim$147 cm^{-1}, and with the C phase (red circles), where the phonon frequency is $\sim$144 cm^{-1}. The gray shaded area highlights a region of coexistence of the 144 and 147 cm^{-1} Tb modes, indicating a coexistence of IC and C phases in this intermediate field region. The inset illustrates Lorentzian fits to the raw 10 K spectrum in the intermediate field regime ($H=6$ T), showing the coexistence of 144 and 147 cm^{-1} Tb modes in this region.

company the magnetic fluctuations as precursors to the IC-C-phase boundary.

We note, finally, that the presence of coexisting IC- and C-phase regions in the intermediate field range $H_c \sim 4$ T $\leq H \leq 7$ T (for $T \ll T_c$) is also supported by the field dependence of the A_g-symmetry Tb-phonon mode. Specifically, this mode exhibits in the intermediate field range a significant linewidth broadening, eventually leading to two-mode behavior—i.e., the presence of distinct peaks at 144 and 147 cm^{-1} associated with the same vibrational mode (see inset of Fig. 5)—consistent with the coexistence of IC- and C-phase regions. The intensity and frequency of the A_g-symmetry Tb mode is summarized as a function of field in Figs. 5(a) and 5(b), respectively. That these two peaks are indeed associated with the same phonon mode is supported by the observation that increasing magnetic field leads to a gradual transfer of spectral weight from the 147 cm^{-1} peak, which is associated with the IC phase, to the 144 cm^{-1} peak, which is associated with the C phase. The appearance of both these peaks in the field range $H_c \sim 4$ T $\leq H \leq 6$ T of $TbMnO_3$ corroborates our other evidence that dynamically fluctuating domains of IC and C phases are present in the intermediate field regime even for $T \ll T_c$.

In summary, our Raman-scattering measurements on $TbMnO_3$ offer evidence that dynamic fluctuations of the field-induced commensurate phase are present outside the established C-phase boundary both for fields $H < H_c$ and temperatures $T > T_c$. These results suggest that the field-induced destabilization of the atomic and magnetic lattices through the IC-C transition in $TbMnO_3$ is associated with the development of fluctuating IC and C domains, which may be instrumental to the field-induced polarization flop from the *c* to the *a* axis. We suggest that these magnetic fluctuations are also accompanied by strong polarization fluctuations that should also be observable as precursors to the field-induced IC-C-phase boundary. Our results also reveal the appearance of additional temperature- and field-dependent modes in the different magnetic phases of $TbMnO_3$ that reflect strong spin-phonon coupling effects, which likely arise from the strong modulation of the exchange interaction by zone-boundary phonon modes. This coupling results in additional modes whose intensities reflect the temperature- and field-dependent sublattice magnetizations of $TbMnO_3$. Finally, our data provides evidence for a structural change that accompanies the field-induced IC-C transition. This structural change is likely associated with an abrupt change in the modulation wave vector of the Tb and Mn ions but x-ray and neutron-scattering experiments would help elucidate the exact nature of this field-induced structural modification.

ACKNOWLEDGMENTS

This material is based on work supported by the U.S. Department of Energy, Division of Materials Sciences, under Award No. DE-FG02-07ER46453, through the Frederick Seitz Materials Research Laboratory at the University of Illinois at Urbana-Champaign, and by the National Science Foundation. Work at Hamburg was supported by the German funding agency under Contract No. RU 773/3-1.

[1] T. Kimura, T. Goto, H. Shintani, K. Ishizaka, T. Arima, and Y. Tokura, Nature (London) **426**, 55 (2003).
[2] T. Arima, T. Goto, Y. Yamasaki, S. Miyasaka, K. Ishii, M. Tsubota, T. Inami, Y. Murakami, and Y. Tokura, Phys. Rev. B **72**, 100102(R) (2005).
[3] T. Kimura, S. Ishihara, H. Shintani, T. Arima, K. T. Takahashi, K. Ishizaka, and Y. Tokura, Phys. Rev. B **68**, 060403(R) (2003).
[4] T. Goto, T. Kimura, G. Lawes, A. P. Ramirez, and Y. Tokura, Phys. Rev. Lett. **92**, 257201 (2004).
[5] M. Kenzelmann, A. B. Harris, S. Jonas, C. Broholm, J. Schefer, S. B. Kim, C. L. Zhang, S.-W. Cheong, O. P. Vajk, and J. W. Lynn, Phys. Rev. Lett. **95**, 087206 (2005).
[6] N. Aliouane, D. N. Argyriou, J. Strempfer, I. Zegkinoglou, S. Landsgesell, and M. v. Zimmermann, Phys. Rev. B **73**, 020102(R) (2006).
[7] F. Bridges, C. Downs, T. OBrien, Il-K Jeong, and T. Kimura, Phys. Rev. B **76**, 092109 (2007).
[8] D. Senff, P. Link, K. Hradil, A. Hiess, L. P. Regnault, Y. Sidis, N. Aliouane, D. N. Argyriou, and M. Braden, Phys. Rev. Lett. **98**, 137206 (2007).
[9] H. Katsura, N. Nagaosa, and A. V. Balatsky, Phys. Rev. Lett. **95**, 057205 (2005).
[10] A. Pimenov, A. A. Mukhin, V. Yu. Ivanov, V. D. Travkin, A. M. Balbashov, and A. Loidl, Nat. Phys. **2**, 97 (2006).
[11] M. Mostovoy, Phys. Rev. Lett. **96**, 067601 (2006).
[12] J. Strempfer, B. Bohnenbuck, M. Mostovoy, N. Aliouane, D. N. Argyriou, F. Schrettle, J. Hemberger, A. Krimmel, and M. v. Zimmermann, Phys. Rev. B **75**, 212402 (2007).
[13] T. J. Sato, J. W. Lynn, Y. S. Hor, and S.-W. Cheong, Phys. Rev. B **68**, 214411 (2003).
[14] J. W. Lynn, R. W. Erwin, J. A. Borchers, Q. Huang, A. Santoro, J.-L. Peng, and Z. Y. Li, Phys. Rev. Lett. **76**, 4046 (1996).
[15] J. A. Fernandez-Baca, P. Dai, H. Y. Hwang, C. Kloc, and S. W. Cheong, Phys. Rev. Lett. **80**, 4012 (1998).
[16] M. Cazayous, Y. Gallais, A. Sacuto, R. De Sousa, D. Lebeugle, and D. Colson, Phys. Rev. Lett., **101**, 037601 (2008).
[17] R. de Sousa and J. E. Moore, Phys. Rev. B **77**, 012406 (2008).
[18] A. B. Harris, Phys. Rev. B **76**, 054447 (2007).
[19] C. S. Snow, S. L. Cooper, G. Cao, J. E. Crow, H. Fukazawa, S. Nakatsuji, and Y. Maeno, Phys. Rev. Lett. **89**, 226401 (2002).
[20] C. S. Snow, J. F. Karpus, S. L. Cooper, T. E. Kidd, and T.-C. Chiang, Phys. Rev. Lett. **91**, 136402 (2003).
[21] Y. Okimoto, R. Kumai, S. Horiuchi, H. Okamoto, and Y. Tokura, J. Phys. Soc. Jpn. **74**, 2165 (2005).
[22] L. Martín-Carrón, A. de Andrés, M. J. Martínez- Lope, M. T. Casais, and J. A. Alonso, Phys. Rev. B **66**, 174303 (2002).
[23] M. N. Iliev, M. V. Abrashev, J. Laverdière, S. Jandl, M. M. Gospodinov, Y.-Q. Wang, and Y.-Y. Sun, Phys. Rev. B **73**, 064302 (2006).
[24] J. Laverdière, S. Jandl, A. A. Mukhin, V. Yu. Ivanov, V. G.

Ivanov, and M. N. Iliev, Phys. Rev. B **73**, 214301 (2006).
[25] T. Kume, T. Hiraoka, Y. Ohya, S. Sasaki, and H. Shimizu, Phys. Rev. Lett. **94**, 065506 (2005).
[26] Th. Rasing, P. Wyder, A. Janner, and T. Janssen, Phys. Rev. B **25**, 7504 (1982).
[27] We note also that the expected coupling of $\mathbf{q}=0$ optical phonons to finite-q spin waves due to zone folding—which is an alternative description of the 125 cm^{-1} IC mode shown in Fig. 3 has also been recently discussed by de Sousa and Moore in the specific case of incommensurate magnetic phases in multiferroic materials; see R. de Sousa and J. E. Moore, Phys. Rev. B, **77**, 012406 (2008).
[28] W. Baltensperger, J. Appl. Phys. **41**, 1052 (1970).
[29] N. Suzuki and H. Kamimura, J. Phys. Soc. Jpn. **35**, 985 (1966); N. Suzuki, *ibid.* **40**, 1223 (1971).
[30] A. Fainstein, P. Etchegoin, H. J. Trodahl, and J. L. Tallon, Phys. Rev. B **61**, 15468 (2000).
[31] X. K. Chen, J. C. Irwin, and J. P. Franck, Phys. Rev. B **52**, R13130 (1995).
[32] G. Guntherodt, W. Bauhofer, and G. Benedek, Phys. Rev. Lett. **43**, 1427 (1979); W. Bauhofer, G. Güntherodt, E. Anastassakis, A. Frey, and G. Benedek, Phys. Rev. B **22**, 5873 (1980).
[33] O. Prokhnenko, R. Feyerherm, M. Mostovoy, N. Aliouane, E. Dudzik, A. U. B. Wolter, A. Maljuk, and D. N. Argyriou, Phys. Rev. Lett. **99**, 177206 (2007).
[34] H. Barath, M. Kim, J. F. Karpus, S. L. Cooper, P. Abbamonte, E. Fradkin, E. Morosan, and R. J. Cava, Phys. Rev. Lett. **100**, 106402 (2008).
[35] D. Senff, P. Link, N. Aliouane, D. N. Argyriou, and M. Braden, Phys. Rev. B **77**, 174419 (2008).